Journal of Environment and Earth Science www.iiste.org
ISSN 2224-3216 (Paper) ISSN 2225-0948 (Online)
Vol. 3, No.10, 2013

Detecting and Quantifying Desertification in the Upper East Region of Ghana using Multi-spatial and Multi-Temporal Normalized Difference Vegetation Index

Owusu, Alex Barimah
Department of Geography and Resource Development, University of Ghana
Legon; P. O. Box LG 59, Legon, Accra-Ghana.
Email: owusuba@yahoo.com

Abstract
The need for process and indicator-based approach for assessing desertification is paramount to the drive to combat desertification in sub-Sahara Africa. It is in line with this that this study sought an approach based on early indicator, which can be measured in a continuum and at multispation and multitemporal scale in order to eliminate short-term phonological variations which are not direct character of desertification in its measurement. The study focused on surface vegetation change trends, as depicted by NDVI, on the African continent, Sahel Africa and the Upper East Region to detect and quantify desertification. The study analyzed NDVI from AVHRR GIMMS NDVIg data (1982-2007) and validated that with Landsat TM5 data (1984-2007). The multitemporal and multispatial validation technique was used to analysis annual temporal and spatial mean NDVI change trends over 26 years. The study finds that temporal NDVI of the African continent has a linear relationship with the seasonal rainfall changes of the year. The mean monthly NDVI for the African region also shows greenness disparity between the northern and southern halves of the continent. It was further observed that mean annual NDVI decrease occurred between 1982 -1983, 1988, 1994, and the largest stretch of decrease expanding over 8 years occurred from 1997-2005. The rise and fall of the NDVI trend from 1982-1997 suggest regular drought on the African continent while the 8-year decrease from 1997-2005 suggests a period of desiccation. These notwithstanding, the NDVI trend of the African continent show no evidence of desertification over the study period. The mean NDVI of the Sahel Africa shows that between 1982 and 1990 NDVI was rising and falling, portraying inter-annual rainfall irregularities of the region. The period 1995-2001 saw NDVI recovering above average, with the highest mean NDVI in 2001. NDVI fell below average from 2002 to 2006. On the average, NDVI of the Sahel Africa increased by about 2.6% during the period under study.
Temporal NDVI of the UER also shows rise and fall trends similar to the Africa and Sahel Africa. However, UER NDVI increased by a higher percentage point 6.7%, as compared to the Sahel Africa average of 2.6% over the 26-year study period. The spatial analysis focused on pixels that lost and those that gained surface greenness over the reference period. The study compared three periods; 1982-1990, 1990-1999 and 1999 - 2007.An average of 19 pixels (8km^2) equals 152 km^2 lost vegetation (1982-1990), while 280 pixels, equivalent to 2240 km^2, gained vegetation. The maximum gain for 1990-1999 was almost 48% of the maximum NDVI for 1987 and 2007. Although GIMMS NDVIg did not find much land degradation, the LTM NDVI shows widespread pockets of spatial degradation in the UER which were not visible in the GIMMS NDVIg. The study concluded that spatial resolution of satellite data changes land degradation dynamics observed in the analysis.
Key Words: Detecting and quantifying desertification, multi-spatial, multi-temporal.

1. Introduction

The number of local and national studies focusing on the subject of desertification demonstrates not only its socio-ecological importance, but also the fact that some parts of the desertification's puzzle remain unsolved (FAO 1999; Veron *et al*., 2006; Geist and Lambin, 2004). The subject lacks an accurate and universally acceptable definition. This disallows scientists the opportunity to assess and measure in universally accepted forms. Various researchers have therefore attempted to measure desertification through a variety of approaches. In measuring desertification, however, there are some controversial issues relating to the nature of the phenomenon. One school of taught argues that it is a state. Another school contends that it is a process. Others even maintain that the reversibility or lack thereof must be the most crucial element for measuring desertification. While delineating the desertification phenomenon, phonological characteristics relating to the "state," "process," and "reversibility or irreversibility" is very useful. They also have implications for policymaking and management. Thus, in deciding on an approach to use for detecting and measuring desertification, one needs to consider these questions. First, is desertification a state or a process? If desertification is considered a state, then one can take a snapshot approach with a single satellite image to detect how it looks. This was the cardinal shortcoming of the first approach to measure desertification by Lamprey (1975) when he attempted to quantify the rate of advancement of the Sahara desert by comparing the location of the southern margins of the Sahara desert at two different times; that is the 1958 margins according to a vegetation map produced by Harrison and Jackson in 1958; and the 1975 margins according to aerial photograph and terrestrial surveys conducted by Lamprey (1975). The author concluded that there was 90–100 km displacement of the margins of the Sahara desert in 17 years, meaning desert edges were encroaching at the rate of 5.5km per year. In reality, desertification is not static; it is a process and changes over time. In Sahel Africa, the presence of vegetative cover is also subjected to inter-annual and inter-decadal and even multi-decadal variations due to rainfall anomalies and sea surface temperature changes. This means that in periods of rainfall anomaly, vegetation declines and recovers sharply when rainfall returns. Plant seeds in these dry land areas could remain dormant for as long as 10 years during periods of drought and desiccation but may revive when conditions improve. Using two dates to map desertification is an over-simplification of the problem because it says nothing about the vegetation status during intervening years. Moreover, it does not take into account interannual and interdecadal rainfall anomalies which can coincide with these two periods of analysis. Prince (2002) argued that desertification needs to be studied as a continuous process for no less than 15 years for any meaningful conclusion.

Secondly, is desertification reversible or irreversible? In this case, if we think desertification is irreversible; then desertification would be seen as desert-like conditions associated with bare surface and severe soil degradation, including gullies. Global Assessment of Soil Degradation (GLASOD) used the extent of soil degradation and the expert opinions of 250 people to assess desertification globally. They combined qualitative and quantitative variables of soil and vegetation and concluded that 70% of all dry lands are affected by desertification. In reality, desertification has phases beginning with degradation of surface cover (vegetation) before reaching the soil (Collado *et al*., 2002; Lu et al., 2004). Desertification process can be halted and reversed depending on the stage of the process; but when it exposes the soil, it is in the advanced stage. Desertification, therefore, has to be assessed in a continuum from the onset to the final state. Initially it is reversible and action must be taken before it reaches the irreversible state. It is against this background that GLASOD's approach to analyzing and monitoring desertification was criticized as autopsy or postmortem by Veron *et al*., (2006) and Prince (2002). Given these methodological complexities any new approach seeking to detect and quantify desertification process must answer the following questions:

- is the approach indicator-based?
- is desertification assessed in a continuum?
- and can the approach be multi-spatially validated?

The need for a process and indicator-based approach for assessing desertification is paramount to the drive to combat desertification in sub-Sahara Africa. However, previous approaches have focused on end-product indicators such as soil degradation. What is missing is that desertification is not necessarily a product, rather a process that has a beginning and an end; hence, the product-based approach leaves much of the quintessential problem of desertification and diminishes the propensity to unravel the mystery of desertification, and above all the likelihood of recovery. By so doing policymakers and practitioners are presented with half the truth about desertification, as we ignore the gist of the desertification problem, origins, and processes. Policymakers and analysts are therefore left with few policy options to address the issue of desertification. It is in line with these that this work focuses on vegetation change trends, as depicted by Normalized Difference Vegetation Index (NDVI) to detect and quantify desertification. By using vegetation change trends, we offer policymakers the option to identify and plan their options before desertification reaches insurmountable levels. Also, the indicator-based approach helps to develop pre-emptive approaches rather than reactive approaches. Front liners have feedback on areas that need more attention and approaches that need to be continued or discontinued by revisiting the indicator that propelled the initial action. This is because we can identify areas of recovery against areas of continual degradation. Another interesting aspect of focusing on NDVI for detecting desertification is the ability to monitor and/or observe in a continuum to avoid the trap of inter-annual/intra-annual and inter-decadal cover changes associated with drought, desiccation, and rainfall anomalies commonly found in the Sahel Africa (Nicholson 1995; 2002).

2. Materials and Methods

The study analyzes NDVI from two different sources. First using Advanced Very High Resolution Radiometer (AVHRR) Global Inventory Modelling and Mapping Studies (GIMMS) NDVI data (1982-2007), 8km spatial resolution, and second using Landsat Thematic Mapper 5 (TP5) NDVI (1984-2007), 30m spatial resolution to analyze the phenological changes (trends) in land degradation over a period of 26 years (1982-2007). The approach monitors changes in NDVI over space and time in order to conclude (confirm or deny) land degradation in the area. This analysis is interested in the annual mean of mean NDVI over the 26 years, annual changes in NDVI in relation to rainfall regimes of the area, and pixel level NDVI regimes over the study period. The pixel level NDVI focused on pixels that have either decreased (degraded) or increased (gained vegetation) NDVI values over the study period of 26 years (1982-2007). The spatio-temporal approach of this study is summarized by the multi-spatial and multi-temporal validation technique shown on Figure 1.

2.1. GIMMS NDVI Dataset

The Global Inventory Modeling and Mapping Studies (GIMMS) data was recorded by AVHRR sensors on 5 satellites of the National Oceanic and Atmospheric Administration (NOAA): NOAA-7, NOAA-9, NOAA-11, NOAA-14 and NOAA- 16. GIMMS data has a spatial resolution of 8 km and a temporal resolution of 15-day maximum NDVI composite. The satellite series NOAA 7, 9, 11, 14 and 16 were used for the International Satellite Land-Surface Climatology Project (ISLSCP) Initiative II NDVI record. The AVHRR satellite series flew in sun-synchronous polar orbits with a nominal overpass 1:30 or 2:30 pm local daytime at launch. However, it has been observed that the overpass times drift by approximately 1-2 minutes per month and reach as high as 4 1/2 hours within the time of recording the data used for this study. This creates variations in illumination and view angles over time. The sensors have a 55 degree swath width, which enables daily view of each pixel on the Earth's surface but at different illumination angles in its 9-day repeat cycle. Maximum NDVI value data composition tends to select pixels which are acquired at near-nadir mode with minimum atmospheric effects; however, illumination and atmospheric effects remain.

GIMMS NDV I datasets used for this study have been generated to provide a nearly 26 year (1982-2007) satellite recording of changes in terrestrial vegetation (Tucker et al., 2005). In spite of numerous shortcomings of NDVI in studying desertification, GIMMS NDVI also called GIMMS NDVIg used in this study was chosen for the following reasons. The GIMMS NDVI dataset from 1982-2007 was prepared with various shortcomings of NDVI in mind. For instance, the dataset has new features including reduction in NDVI variations occurring from sensor calibration, view geometry, volcanic aerosols, and other effects not related to actual phenological changes of interest to this study (GIMMS NDVIg documentation 2004). Specific cases include the NOAA-9 (sensor) descending node data from September 1994 to January 1995, which was known to have been affected by volcanic stratospheric aerosol, and was corrected from the affected datasets, 1982-1984 and 1991-1994. Also, NDVI was improved using Empirical Mode Decomposition/reconstruction (EMD) to minimize effects of orbital drift (Pinzon et al., 2004; 2002). The GIMMS NDVIg was originally produced as a global NDVI to provide inputs for computing the time series of biophysical parameters contained in the International Satellite Land Surface Climatology Project (ISLSCP) Initiative II collection (Tucker *et al*., 2005). However, GIMMS NDVI has been used and/or tested for climate and biogeochemical modeling to calculate photosynthesis, the exchange of CO_2 between the atmosphere and the land surface, land-surface evapotranspiration and the absorption and release of energy by the land surface (Hall et at 2006; Hu et al., 2008; Karlsen et al., 2005; Tucker et al., 2005; Pinzon et al., 2004; 2002).

The GIMMS NDVI data is of coarse resolution on a global scale with a spatial resolution of 8km. However, the decision to use AVHRR GIMMS data, in addition to its relevance and also the fact that some of the identified shortcomings have been addressed, is based on long term data availability and accessibility, which is necessary for the study of desertification (Prince *et al*., 1998; Veron *et al*., 2006). Also, AVHRR NDVI data is useful for analyzing changes in vegetation cover over a long period. Again, GIMMS NDVI becomes useful to this study for the fact that detailed observation and analysis of identified degraded pixels can be verified and validated with Lansat TM5 data of 30m, a medium resolution. Furthermore, several studies attest to the fact that GIMMS NDVI performs far better, in terms of vegetation monitoring, than AVHRR pathfinder data (Tucker et al., 2005; Hall et al., 2006; Hu et al., 2008; Karlsen *et al*., 2005).

The AVHRR flown on NOAA-14 and previously on NOAA-7, NOAA-9, and NOAA-11, has 5-channel instruments, which scan continuously at a ground resolution of 1 km. The 1 km data has been re-sampled and averaged to nominal 8 km resolution GIMMS NDVI data. AVHRR Global Area Coverage (GAC) at 8 km resolution is available at no cost. AVHRR sensors acquire data in 5 spectral bands: band1-the visible, band2-the near infrared and the remaining three bands (bands 3, 4, and 5) in the thermal region. The GIMMS NDVI data does not make use of the three thermal bands. The spectral ranges of the five AVHRR channels are contained in Table 1.

The spectral bands commonly used for vegetation monitoring are the Channel 1 visible band (0.58 to 0.68 micrometers) and Channel 2 in the near infrared band (0.725 to 1.0 micrometers). The spectral response curves for these channels are said to be similar to those of bands 5 and 7 on the Landsat satellite (Tucker et al., 2005). The mathematical combinations of Channel 1 and 2 data are found to be sensitive to the presence of green vegetation and are therefore called vegetation indices. This is mainly due to the differential reflectance of vegetation in these wave bands. The differences in Ch2 and Ch1 data values, computed as Ch2-Ch1, is an indicator of the degree to which the Instantaneous Field Of View (IFOV) being sensed includes green vegetation. The vegetation index of interest to this study is the Normalized Difference Vegetation Index (NDVI). The NDVI is defined by the equation:

$$NDVI = \frac{Ch2-Ch1}{Ch2+Ch1} \quad (1)$$

The NDVI is mostly preferred for global vegetation monitoring mainly due to partially compensating for changing illumination conditions, surface slope, and viewing aspects (AVHRR online documentation 09/04/08). Clouds, water, and snow have larger reflectance in the visible band than in the near infrared band, so for these features, NDVI is negative. Rock and bare soil have similar reflectance in these two bands and result in vegetation indices near zero. In scenes with vegetation, the NDVI ranges from 0.1 to 0.6; higher values are associated with greater density and greenness of the plant canopy.

2.2 The Landsat Dataset

The GIMMS NDVI dataset was supplemented with seven Landsat Thematic Mapper 5 (LTM5) data. The Landsat mission was first launched on July 23, 1972. The first Landsat satellite carried on board two instruments that look at the Earth's surface--the Return Beam Vidicon (RBV) and the Multi-Spectral Scanner System (MSS). The original satellite was called the Earth Resources Technology Satellite (ERTS-1) and later became Landsat-1, followed by Landsats-2, -3, -4, -5, and -7. Landsat-6 failed at launch.

The RBV and MSS were flown on all the first three Landsat satellites. Landsat 4 and 5 had MSS and the Thematic Mapper (TM). Landsat-6 was equipped with the Enhanced Thematic Mapper (ETM) and Landsat-7 carried the Enhanced Thematic Mapper-plus (ETM+). The operating dates of Landsat satellites and instruments they carried on board are listed in Table 2.

The TM instrument on board Landsat 4 and 5 and the ETM+ on Landsat-7 view the Earth’s surface with 7 spectral bands. The bands 1, 2, 3, 4, 5,0 and 7 are sensitive to light from the sun reflected by Earth surface targets. Each band focuses on different parts of the reflected portions of the electromagnetic spectrum. The parts of the electromagnetic spectrum (EMS) are defined by the wave length of the light waves. Band 1 of the TM and ETM+ instruments records in the wave length range of 0.45- 0.52 microns (μm) (the blue portion of the spectrum). Also, bands 2 and 3 of the TM and ETM+ instruments record reflected green and red light, respectively. TM and ETM+ bands 4, 5, and 7 record reflected light in the infrared portions of the spectrum, specifically near infrared (NIR, band 4) and short wave infrared (SWIR, bands 5 and 7). Unlike the other bands, band 6 of the TM and ETM+ instruments record heat energy emitted by the Earth's surface in the thermal band of the EMS. In addition to the reflected and thermal bands, the ETM+ instrument of Landsat-7 has an eighth band, the panchromatic band. ETM+ band 8 is sensitive to reflected light energy across a broad range of wavelengths that includes blue, green, red, and near infrared. Unlike the other bands, band 8 of the ETM+ has a spatial resolution of 14.25 meters, instead of the 28.5 meters of bands 1, 2, 3, 4, 5, and 7. The sensitivities of Landsat instruments (RBV, MSS, TM, and ETM+) and bands are listed in Tables 3 and 4.

This study used seven Landsat TM5 images (1982-2007) cloud free (0% cloud cover) surface reflectance data with a spatial resolution of 30m. The decision to use seven TM5scenes was based on data availability at the right conditions and the fact that the greater part, if not all of the study area falls within one Landsat scene path 194 and row 053. The selection of the 7 scenes was done carefully to avoid phenological changes in vegetation caused by seasonal variations. The study therefore selected 7 scenes in October/November as illustrated in Table 5.

In addition, data has been selected to take care of intra-seasonal phenological variations related to local seasonal variability due to rainfall, agricultural harvest, and bush burning. The month of October/November was selected because it is the period just after the raining season and before the onset of the dry season. It is also a period before local bush burning for hunting, grazing, fire festival, and agricultural purposes. Furthermore, October/November marks the end of agricultural harvesting in the UER. By selecting data from the month of October/November and near anniversary dates, phenological variations would be normalized (Lunetta et al., 2002; Lu et al., 2004; Coppin et al., 1996). The high spatial resolution of Landsat TM5data make them suitable for this study, since it can capture almost all major local variation in land degradation (Collado et al., 2002). Various studies have attested to the spatial variability in degradation and causative agents, which have also been the basis of criticism for some earlier attempts at quantifying and analyzing desertification globally (Veron et al., 2006). Local variations and causes are very important not only to this study, but also for any attempt to combat desertification locally. The LTM5 data is also useful for validation of AVHRR data.

Landsat images used in this study were obtained from the United States Geological Service (USGS) Center for Earth Resources Observation and Science (EROS) data center at Sioux Falls, South Dakota, with support from the Borlaug-LEAP Grant administered by the Leadership Enhancement in Agriculture Program (LEAP); University of California Davis (UC Davis); and the International Food Policy and Research Institute, Washington, D.C.

The data was radiometrically and geometrically corrected at the source and the digital numbers were converted to radiance and to reflectance. This reduced processing time and cost and ensured timely completion of the study. However, further normalization was performed to correct for atmospheric effect using the FLAASH image normalization package in the ENVI 4.7.1 software. Image processing steps followed in this study were:

i. The seven Landsat scenes were co-registered using image to image registration package in the ENVI 4.7.1 software.
ii. Image subsetting – Landsat image is 185x185 km; meanwhile, the study area is approximately 160x120, so there was the need to subset the image to the region of interest (study area). For the purpose of subsetting, the images were projected to the same projection as the shapefile of the study area (UTM zone 30) with Datum NAD WGS84. The images were overlaid with the study area boundary shapefile in ENVI 4.7.1 software. The images were subsetted to cover the study area.
iii. NDVI processing: ENVI 4.7.1 software was used to process NDVI through Idl band math functionality. Band math is a mathematical approach that performs mathematical operations on an image based on selected mathematical operations.
NDVI is an index ascribed to Rouse et al (1973), although the concept of a normalized difference index is said to have been first introduced by Kriegler and others in 1969 (Ray 1994). NDVI has the advantage of varying between -1 and 1, with 1 indicating the maximum and -1 the minimum.
NDVI was calculated as:

$$IDL\ NDVI = \frac{(float(b1) - float(b2))}{(float(b1) + float(b2))} \quad (2)$$

Where, b1 represents Landsat band 4 (NIR) and b2 represents band 3 (Red) and float converts the image from byte to a floating number.
iv. Image inspection and further validation with GPS locations taken from the field during the field validation (December 07-February 08).
v. Generation of NDVI values for the degraded pixels of the AVHRR data.
Plotting of GIMMS NDVI degraded pixel values into a line graph over the study period.
Essentially, using two different sensor images of different spatial resolutions allowed two levels of analysis from coarse to medium spatial resolution. The two levels of analysis can also be understood as pixel level analysis (8km), which equates 266 Landsat pixels. The study performed trend analysis on annual mean NDVI levels using GIMMS NDVI and compared that to the NDVI generated from seven single scene images of LTM5. The study further validated the observations from GIMMS NDVI and LTM5 scenes with GPS location data for degraded communities. The steps for image processing are depicted in Figure 2.

3. Results and Discussions

3.1 NDVI as Desertification Indicator on the African Continent

Vegetation greenness measured in terms of NDVI on the African continent has a linear relationship with the seasonal changes of the year. Greater parts of the African continent, particularly sub-Sahara Africa which stretches from the southern borders of the Sahara Desert to the northern borders of South Africa and Namibia, due to its tropical location and near constant temperature, have their seasons determined by rainfall. As such, there are two main seasons, the rainy season and the dry season. During the northern summer, when the sun is in the northern hemisphere, the ITCZ moves north of the equator to create a low pressure belt, which brings the African monsoon winds to the northern parts of the continent. This is the period from March 21st to September 23rd, hence NDVI increases in the northern parts of the continent from March to September, thus representing northern summer or the rainy season (see Figure 3). Conversely, the sun apparently relocates to the southern half of the continent from October to February, which relocates the ITCZ to the southern half of the continent to attract moisture-loaded winds to create a rainy season in this part of the continent. For this reason, seasonal NDVI from the African continent shows two peaks, March-September for the northern summer, also the rain season in the North, and October-February for the southern summer, which is also the rain season in the South as shown in Figure 3. In Figure 3, the y-axis indicates mean monthly NDVI values from 1982 to 2007 and the x-axis indicates months of the year, from January to December.
The mean monthly NDVI for the African region also shows greenness disparity between the northern and southern halves of the African continent. The temporal NDVI from 1982-2007 shows a general trend of rise and fall every two to three years. NDVI declined from 1982 to 1983 and rose from 1984 to 1986 and then declined again. There are 4 peaks occurring from 1984-1986, 1989-1991, 1996-1997, and 2004-2007. Periods of low NDVI observed in the 26 years NDVI analysis include 1982-1983, 1988, 1994, and the largest stretch of periods with low NDVI expanding over a period of 8 years from 1997-2005. The rise and fall of the NDVI trend from 1982-1997 suggest regular drought on the African continent. Drought occurs naturally and lasts over a short-term (1±2 years) when precipitation is significantly below normal recorded levels. It is also referred to as the inter-annual rainfall variability, a common phenomenon on the African continent. Normally green vegetation wither during periods of drought to conserve available water to ensure survival, hence the absence of green leaves. This is indicated by decreased NDVI, but vegetation recovers rapidly after the rain returns, hence increased NDVI trend. The 8-year period from 1997-2005 of NDVI trend shows continuously low NDVI trend,

suggesting a period of desiccation. Darkoh (1998) describes desiccation as a period of extended drought lasting up to a decade. Usually, desiccation describes periods when drought extends between three and ten years, as in the case of the period spanning 1997-2005.

It is, however, important to caution that on a continent as large as Africa; desiccation may be a sub-regional or some stochastic local phenomena but can have impact (regional and sub-regional effect) on the general NDVI trend of the entire continent. The NDVI trend from 1982-2007 from the African continent shows no evidence of desertification. Desertification manifests itself in the form of progressive reduction of NDVI over a period of no less than 15 years. Also, NDVI can be rising and falling at the same time, yet it may be below the general average of the period under investigation, which is evidence of desertification. However, there is also no strong evidence to negate the fact that desertification can be taking place in some parts of the continent. The NDVI analysis of the African continent includes regions of tropical rainforest and desert land where desertification is practically impossible. The general conclusion from observing NDVI trend on the African continent is that NDVI shows the expected inter-annual and inter-decadal variations from 1982-1997, followed by 8 years of decline, signifying desiccation from 1997-2005. However, there is evidence of recovery since 2005 from the observed desiccation from 2005-2007. Whereas there is no evidence of desertification for the entire African continent, the study isolate a region within the dry sub-humid, arid, and semi-arid regions where desertification is more likely to occur for detail analysis. In the next paragraph critically analyze Sahel region to determine if there were possible signs of desertification from 1982-2007.

3.2. NDVI and Desertification in the Sahel Africa

In refocusing our discussions on desertification, the study analyzes NDVI of the Sahel Africa, where the likelihood of land degradation is higher. In order to be consistent with other earlier studies, this study define Sahel Africa coterminous to Tucker et al., (1991), as the region between latitude 10^o N and 25^o N and longitude 16^o W and 39^o E (see figure 6 below). Characteristically, the Sahel Africa falls within the arid, semi-arid, and the dry sub-humid regions north of the equator where desertification normally occurs. In the southern parts of the Sahel Africa (around latitude 10^o N), annual rainfall is as high as 1100mm. However, in the extreme North, the annual rainfall can be as low as 300mm. Rainfall duration ranges from 5 months in the South to as low as 3 months in a year in the North. It is also characterized by torrential rains and flash flooding.

The NDVI regime of the Sahel Africa is no different from the rest of the continent; it coincides with the rainy season that peaks in September. The NDVI rises from May to September and declines sharply in October, until it reaches the minimum in March. Sahel Africa has a single rainfall maximum (monomodal rainy season), which lasts for a few (about 5) months, from April/May to September/October and a long dry season from October/November to March/April, depending on the latitudinal location. The mean NDVI for the Sahel Africa shows unique and interesting characteristics that worth analyzing. Studies conducted in the region over the 1980s and early 1990s sang the praises of Sahel greening; however, the same mean NDVI (1982-2007), as in this study figure 5 and 6 below shows that the Sahel greening was subjected to spatial and temporary irregularities. The period 1982-1990 saw NDVI rising and falling (figure 5), portraying (responding to) the inter-annual rainfall irregularities of the region, though generally on the rising side.

However, the period 1990-1994 saw 4 years of continuous decline in NDVI below average, showing a decrease of about 5.4%, which signifies a period of desiccation. 1995-2001 saw NDVI recovering above average, with the highest mean annual NDVI in 2001. This is followed by another five years of falling NDVI below the period average 2002-2006. Generally, NDVI in the Sahel region has been on the positive side, showing an average increase of 2.6% over the 26-year period from 1982-2007, with 1982 as the base year.

3.3. Temporal NDVI for Desertification in the UER

Located between latitude 10.40 N and 11.5 N and longitude 1.36 W and 0.09 E, the UER forms part of the Sahel Africa. It falls within the dry sub-humid portions of the Sahel with an annual rainfall of about 1100 mm. The seasonal trend of NDVI in a normal year for the UER shows a gradual rise from April, peaks in September and declines gradually from late October and reaches its minimum in February. The normal seasonal NDVI trend in the UER is shown in Figure 7. This is similar to the normal trend of NDVI in the Sahel West Africa. However, in abnormal years, which would simply be interpreted as drought years, the NDVI trend would look different, corresponding to the timing of the rain in the locality of interest.

Twenty-six years mean NDVI, composed of a 15-day average composite from 1982 to 2007 and plotted to time-series NDVI for the UER is presented below. Figure 8 below is the mean NDVI map for 2001, covering the UER. The NDVI indicates that greenness in the region has increased steadily, after starting lows of what appears to be drought years of 1982, 1983, and 1984. It also shows the regular cycle of NDVI fluctuations linked to rainfall anomalies associated with the study area. From the period 1982 to 2007, vegetation greenness measured in terms of mean NDVI rose steadily from an annual mean of about 0.37 in 1982 (the base year) to about 0.45 in 2007, the end year. This indicates a positive NDVI change of about 21.6% over a period of 26 years. On the average, NDVI increased by about 6.7% from 1982-2007. The NDVI of the UER also shows a similar rise and fall trend as in the Africa and Sahel Africa NDVI, of which the UER forms a part. However, there are some important differences between the NDVI of the UER and the Sahel Africa. First, NDVI has increased by a higher percentage point in the UER with an average of 6.7%, against the Sahel average of 2.6% over the 26-year study period.

Secondly, whereas the Sahel Africa NDVI shows signs of desiccation from 1990-1994 and 2002-2006, the UER NDVI does not show any signs of desiccation, drought nor desertification, suggesting that there were no climate anomalies in the UER in those same years, with the exception of the starting years of 1982-1984, which of course form the base years for comparison.

The NDVI trend of the UER confirms to the general observations of previous studies that the Sahel Africa is getting greener. What the study cannot say is whether desertification had taken place prior to 1982, the base year for this study, in order to think of recovery. As far as it can be ascertained from the NDVI observations (1982-2007), there were no indications of desertification; rather, there were significant increase in surface greenness, averaging about 6.7%, a percentage point well above the Sahel Africa average of 2.6% and the Africa average, which saw a decrease of about -0.04%.

3.4. Spatial Variability of NDVI in the UER

Having extensively looked at the temporal dynamics of NDVI, this section looks at the spatial dynamics of NDVI in the UER. The focus of this section was to analyze how NDVI has changed spatially. The study analyzed the pattern of NDVI changes by comparing three spatio-temporal ranges, expanding from 1982-1990, 1990-1999, and 1999-2007. The analysis focused on spatial NDVI losers and gainers, i.e. pixels that lost surface greenness and those that saw an increase in surface greenness over the reference period. From 1982 to 1990, an average of 41 pixels of 8km^2 each, which converts to 328 km^2 lost greenness in the UER. Conversely, land area of approximately 2064 km^2 gained or showed increase in surface greenness. The period 1990 to 1999 saw 102 pixels (816 km^2) losing its surface greenness, while 197 pixels (1576 km^2) gained greenness. However, more land area lost surface greenness from 1990-1999 than the period 1982-1990. Areas that lost vegetation were concentrated around the south-west, and south-central portions of the study area. Compared to 1982-1990 and 1990-1999, the period 1999 to 2007 lost less vegetation. An average of 152 km^2 lost vegetation, while 280 pixels, equivalent to 2240 km^2, gained vegetation. Whereas 1999-2007 had the lowest number of pixels losing greenness, the period 1982-1990 had the highest gain in greenness; the period 1990-1999 had both the highest number of pixels losing greenness, and at the same time, the minimum gains in vegetation greenness. On the average, the period 1982-1990 gained more green vegetation than a single year maximum NDVI for 1983, 1984, and 1985.The maximum gain for 1990-1999 was almost 48% of the maximum NDVI for 1987 and 2007, and the maximum gain for 1999-2007 is greater than the yearly mean NDVI recorded over the 26-year period. In general, surface greenness increased from 1982 to 2007, indicated by the positive mean gains for 1982-1990; 1990-1999; and 1999-2007, confirming the observation from the temporal NDVI trend that surface greenness, as depicted by the NDVI, shows greening of the UER from 1982-2007. The mean pattern of spatial NDVI gainers and losers are summarized in Figure 9.

The spatial pattern of gainers and losers show that more pixels in the eastern and central portions of the study area gained vegetation, while south western portions of the study area lost more vegetation from 1999-2007. The overall mean gains and losses show that land degradation is not uniform in the UER, nor does it occur at the same rate. It is against this background that we conclude that land degradation is more likely to be a function of land use, in terms of frequency and intensity than climate, although climate impact cannot be wholly exonerated.

3.5. NDVI for Desertification Analysis Using LTM5 for the UER

The accuracy of GIMMS' NDVIg for monitoring surface greenness has been validated from several studies, including Tucker et al., (2005), Hall et at (2006), Hu et al., (2008), and Karlsen et al., (2005). However, this study was interested in the differences in NDVI trend of medium and coarse resolution satellite data. The study therefore gathered LTM5 data with spatial resolution of 30m, compared to 8km by GIMMS NDVI. Within the limits set by available LTM5 data, the study analyzed the NDVI trend from seven LTM5 scenes, specifically scenes captured in the months of October/November, in order to avoid phenological changes due to seasonal changes in NDVI. The result is depicted in Figure 10.

LTM NDVI shows that the UER is generally sparsely vegetated with a few clusters of heavily vegetated areas and several exposed areas. Green vegetated areas are mostly found along river banks forming corridors. Some studies, including Dietz and Millar (1999) and the Regional Coordinating Council (2005), have indicated that areas along river banks were infested with black flies which cause onchocerciasis (river blindness) and therefore not favored for human usage. Also, the ever-greenness of vegetation along river banks makes it difficult to burn, compared to other areas that dry out completely and therefore become susceptible to annual burning. Figure 11 is the NDVI map of the UER from LTM5. Statistics computed from LTM5 images show that the average vegetation of the areas rose by about 100% between October 20, 1984 and October 30, 2002, using October 20, 1984 as the baseline, while on the average, NDVI increased by about 29.7%.

Even though the temporal analysis of LTM5 NDVI indicates rising trends, spatial analysis shows widespread pockets of degradation in the area. Change detection performed of LTM5 images of 1999 and 2002 show that degradation occurred between the two time periods in the eastern and central portions of the study area. It also shows urban expansion in the Bolgatanga, Navorongo, and Paga areas as shown on Figure 11. The map shows areas of greening, indicated on the map by green, areas of no change between the two time periods indicated by white color, and areas of degradation indicated by brown color.

The LTM5 NDVI equally shows greening, it shows more degradation of the area than the GIMMS NDVI. This difference in spatial pattern of degradation raises the question of scale. It therefore becomes pertinent for remote sensing NDVI based study of desertification to answer the question of scale, both temporal and spatial. Temporal analysis in highly variable areas such as the UER and Sahel region in general must be considered very important in drawing conclusions. Vegetation in this part of the earth is highly contingent on rainfall pattern. In the UER residential neighborhoods of urban centers turn green fields during the rainy and agricultural growing seasons as most people turn their backyards into full-fledged farms. However, backyards turn into grazing and burnt fields during the post-harvest periods, hence the timing of data acquisition becomes very important and make the difference between green fields and degraded land. Furthermore comparison between LTM NDVI, and GIMMS NDVIg underscores the need for high spatial resolution data for analyzing desertification in the UER. It is observed from the field study conducted, that the principal driver of land degradation in the UER was the use of fire for farming and other agricultural purposes. However, the average farm size in the region is 3-5 hectares, which converts to 0.03 to 0.05 km^2 whereas the pixel size of the GIMMS data used is 8 km^2; it is therefore not surprising that much of the degraded areas tends to be absorbed and averaged out in the broader picture to show much greener areas. On the other hand, medium resolution LTM5 data, 0.03km^2, which is about the average farm size in the UER, is able to depict pockets and clusters of degraded lands much better as shown on Figure 11. Some of the common reasons for land degradation include land extensification (increasing production by cultivating more land) to marginal lands such as areas previously infested with black flies, which causes river blindness. Some Ministry of Food and Agriculture (MoFA) officials interviewed in this study spoke of the recent eradication of black flies from some river valleys, making those areas suitable to cultivation and grazing. Increasing agricultural activities and urbanization have also played an important role in land degradation in the UER.

4. Conclusions and Recommendations

Although a great deal of data on land resources is available, it has not been possible to get a clear picture of the status of desertification at regional or national levels (UNCCD, 2000). This study provides a clearer picture of the status of desertification in the UER, taken inspirations from other studies including Lamprey (1975) and Prince *et al*., (1998). Considering the importance of desertification to residents of the UER and dryland regions of Africa whose survival are tied to dryland vitality, it is imperative that scientists build consensus and collaborate to provide accurate information and credible methodology for its assessment. Since the Stebbing's pioneering work on desertification in 1935, several other works, providing different estimates using different methodologies have surfaced and have been critiqued in the literature. Notwithstanding the unfavorable reviews by some scholars in the field, these works have shaped and improved the direction of the discourse and contributed to the methodological development over the years. Two prominent of these studies that have received much attention and reviews in the literature and have also contributed tremendously to the current debate on desertification are the study by Lamprey (1975) in southern Sudan and Prince *et al*., (1998) in the Sahel region of Africa. These studies vary both in time and space, hinging on different perceptions which directed the methodological approach and conclusions, their points of divergence and convergence have proven to be the strength of many current desertification studies including this study.

On the basis of these studies and their numerous critics**,** this study was framed to advance knowledge on contentious issues such as static versus dynamic, reversibility versus irreversibility, spatial and temporal scales and more importantly the need for long term study. Analysis of NDVI from GIMMS data shows that the NDVI from the Sahel region 1982-1990 projected a strong rising trend, however, the periods after 1990; more especially the period from 2001 to 2006 shows a disturbing declining trend. This reinforces the call for long–term analysis in order to make a very conclusive argument.

Whereas long–term and continuous analysis is important, we also find that spatial pattern of degradation may contradict temporal patterns. The spatial pattern of degradation shows moderate to severe localized degradation areas of Senegal, southern Sudan, Niger, and Mali (see Figure 8). We therefore concluded that although the general surfaces appearance is important, localized degradation tends to be overlooked, and this raises question of scale. Prince *et al*., (2007) stated that one major problem with RUE is the difficulty of computing RUE over the entire Sahel region. Comparing GIMMS NDVIg of 8km resolution with LTM5 NDVI of 30m resolution, the study find a widespread pockets of degradation in the LTM5 NDVI of the UER which were not captured in the

GIMMS NDVIg, hence spatial resolution of data changes land degradation dynamics observed in the analysis. The study therefore concluded that Lamprey (1975) made a very important contribution to methodological development; however, he fell short in terms of viewing desertification as static and irreversible. Prince *et al.*, (1998) responded to the need for practical, objective methodology based on indicators, however, their study did not have long-term data and also did not account for localized land degradation, which creates localized impact on communities, regions, and countries. Future studies should therefore look into temporal and spatial scale differentials or impacts.

References

Aubreville, A., (1949). Clamats, forests et desertification de l' Afrique Tropicale Societe de Editions Geographiques. Maritimes et Coloniales Paris

AVHRR Online Documentation (2005) http://noaasis.noaa.gov/NOAASIS/ml/avhrr.html

Collado, A. D., Chuvieco, E. and Camarasa, A., (2002). Satellite Remote Sensing analysis to monitor desertification process in crop-rangeland boundary of Argentina. Journal of Remote Sensing, Vol. 52: 121-133

Coppin, P. R. and Bauer, M. E., (1996). Change Detection in Forest Ecosystems with Remote Sensing Digital Imagery. Remote Sensing Reviews 13:207-234 (1996)

Darkoh, M.B.K., (1998). The nature, causes and consequences of desertification in the drylands of Africa. Land Degradation and Development, 9 (1), 1–20.

Dietz, T. and Millar, D. (eds), (1999). Copping with climate change in dryland Ghana. The case of Bolgatanga. Netherlands Research Program on Climate Change, Amsterdam.

Diouf, A. and Lambin, E. F., (2001). Monitoring land-cover changes in semi-arid regions: remote sensing data and field observations in the Ferlo, Senegal Journal of Arid Environment

Dregne, H. E., (1986). Desertification of arid lands. In El-Baz, F. and Hassan, M. H. A. (ed.).Physics of desertification. Dordrecht, Netherlands: Martinus, Nijhoff.

Food and Agricultural Organization of the United Nations (1999). Report for the third conference of parties of the Convention to Combat Desertification.

Geist H. J. and Lambin E.F., (2004). Dynamic Causal Patterns of Desertification. BioScience.September 2004 / Vol. 54 No. 9

Hall, F., Masek, J.G. and Collatz G. J., (2006). Evaluation of ISLSCP Initiative II FASIR and GIMMS NDVI products and implications for carbon cycle science. Journal of Geophysical Research, Vol. 111, D22S08, doi:10.1029/2006JD007438, 2006

Hein L. and de Ridder, N., (2006). Desertification in the Sahel: a reinterpretation. Global Change Biology (2006) 12, 751–758

Helldén, U., (1991). Desertification – Time for an assessment. Ambio 20: 372-383

Holm, A.M., Cridland, S.W., Roderick, M.L., (2003). The use of time-integrated NOAA NDVI data and rainfall to assess landscape degradation in the arid shrub land of Western Australia. Remote Sensing of Environment 85,145–158

Hu, Y., Ban, Y., Zhang Q., Hu, Y. Zhang, X., J. Liu, and Zhuang D., (2008). Spatial–Temporal Pattern of GIMMS NDVI and Its Dynamics in Mongolian Plateau. 2008 International Workshop on Earth Observation and Remote Sensing Applications. IEEE.

Karlsen S. R., Elvebakk A., Høgda K. A., Johansen B., Beck P. S. A., (2005). GIMMS-NDVI based mapping of the growing season and bioclimatic zones in Fennoscandia and neighboring parts of NW Russia. Proceeding (extended abstract) for the 31st International Symposium on Remote Sensing of Environment (IRSE). 20-24 June 2005, Saint Petersburg, Russian Federation

Lambin E.F., et al.,. (2001). The causes of land-use and land-cover change: Moving beyond the myths. Global Environmental Change 11: 261–269.

Lamprey, H. F., (1975). Report on the desert encroachment reconnaissance in northern Sudan, 21 Oct. to 10 Nov. UNESCO/UNEP 16 pp

Lunetta, R. S., Ediriwickrema, J., Johnson, D. M., Lyon, J. G., and McKerrow A., (2002). Impacts of vegetation dynamics on the identification of land-cover change in a biologically complex community in North Carolina, USA. Remote Sensing of Environment 82 (2002) 258–270

Lu, D., Mausel, P., Brondizio, E. and Moran, E., (2004). Change detection techniques. Int. J. Remote Sensing, Vol. 25.No. 12, 2365-2407

Mainguet, M. and Da Silva, G. G., (1998). Desertification and Drylands Development: What Can Be Done? Land Degradation and Development, Volume 9 Issue 5, Pages 375 - 382

Nicholson, S. E. (1995). Variability of African Rainfall on Interannual and Decadal Time Scales, *Natural Climate Variability on Decade-to-Century Time Scales,* National Academy Press, Washington D. C.

Nicholson, S., (2002). What are the key components of climate as a driver of desertification? In Global Desertification: Do Humans cause Desertr? (Ed) Reynolds, J.F. and Stafford Smith D.M.. Dahlem University Press

Nsiah-Gyabaah, K., (1994). Environmental Degradation and desertification in Ghana. Ashgate Publishing Limited, Vermont USA

O'Connor, T. G., Haines, L. M., Snyman, H. A., 2001. Influence of precipitation and species composition on physical to mass of semi-arid African grassland. Journal of Ecology 89,850

Pinzon, J., (2002). Using HHT to successfully uncouple seasonal and interannual components in remotely sensed data. SCI 2002. Conference Proceedings Jul 14-18. Orlando, Florida.

Pinzon, J., Brown, M. E. and Tucker, C. J., (2004). Satellite time series correction of orbital drift artifacts using empirical mode decomposition. In Hilbert-Huang Transform: Introduction and Applications, eds. N. Huang, pp. Chapter 10, Part II. Applications

Prince, S.D, Brown De Colstoun, E. and Kravitz, L.L., (1998). Evidence from rain-use efficiencies does not indicate extensivlian desertification. Global Change Biology, 4, 359-374

Prince, S.D. (2002). Spatial and temporal scales for detection of desertification. In: J.F. Reynolds and D.M. Stafford Smith, Editors, *Global Desertification: Do Humans Create Deserts?*, Dahlem University Press, Berlin.

Prince, S. D., Wessels, K. J., Tucker, C.J. and Nicholson, S. E., (2007). Desertification in the Sahel: a reinterpretation of a reinterpretation. Global Change Biology Volume 13, issue 7; pp. 1308-1313

Ray, T. W., (1994). A Frequently Asked Questions (FAQ) on Vegetation in Remote Sensing. Written by Div. of Geological and Planetary Sciences. California Institute of Technology.Pasadena, CA Regional Coordinating Council, (2005). Upper East Region: Over view. RCD Bolgatanga.

Rouse, J.W., Haas, R.H., Schell, J.A. and Deering, D.W. (1973). *Monitoring Vegetation Systems in the Great Plains with ERTS*. Third ERTS Symposium, NASA SP-351 I: 309-317.

Stebbing, E.P., (1935). The encroaching Sahara: the threat to the West African colonies, *Geographical Journal* **85**, pp. 506–524.

Thomas, D.S.G., (1997). Science and the desertification debate, *Journal of Arid Environments* **37**, pp. 599–608

Tucker, C.J., Dregne, H.E. and Newcomb, W.W., (1991). Expansion and contraction of the Sahara desert from 1980 to 1990, *Science* **253**, pp. 299–301

Tucker, C. J., Pinzon, J. E., Brown, M. E., Slayback, D., Pak, E. W., Mahoney, R., Vermote, E. and El Saleous, N., (2005). An Extended AVHRR 8-km NDVI Data Set Compatible with MODIS and SPOT Vegetation NDVI Data. International Journal of Remote Sensing

UNCCD, (2000). Assessment of the status of land degradation in arid, semi-arid and dry sub-humid areas. United Nations Convention to Combat Desertification, Bonn.

Verón, S.R., Paruelo, J.M. and Oesterheld, M., (2006). Assessing desertification. ***Journal of Arid Environments;*** Volume 66, Issue 4, September 2006, Pages 751-763

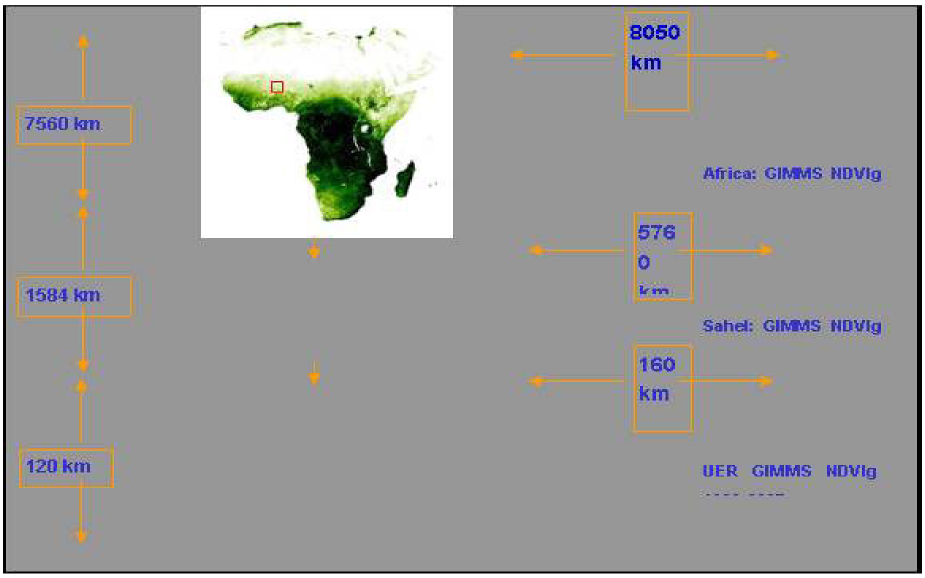

Figure 1: Multi-spatial NDVI Analysis

Table 1: Range of Spectral Values for AVHRR Channels

AVHRR Ch. Number	Range (micrometers)
1	0.58 - 0.68
2	0.725 – 1.0
3	3.55 - 3.93
4	10.30 – 11.30
5	11.50 – 12.50

Table 2: Landsat Satellites, their Operational Periods, and their Instruments

Spacecraft	Launched	Out of Service	Instruments
Landsat-1 (ERTS-1)	July 23, 1972	January 6, 1978	RBV, MSS
Landsat-2	January 22, 1975	February 25, 1982	RBV, MSS
Landsat-3	March 5, 1978	March 31, 1983	RBV, MSS
Landsat-4	July 16, 1982	June 15, 2001	MSS, TM
Landsat-5	March 1, 1984	Operational	MSS, TM
Landsat-6	October 5, 1993	October 5, 1993	ETM
Landsat-7	April 15, 1999	Operational	ETM+

Table 3: Landsat 1-5 Instruments and Bands

Channel	RBV Spectrum	RBV Pixel Size	MSS Spectrum	MSS-Pixel Size
1	.48-.57 µm green	79 meters, 1.5 acres	N/A	N/A
2	.58-.68 µm red	79 meters, 1.5 acres	N/A	N/A
3	.69-.83 µm IR	79 meters, 1.5 acres	N/A	N/A
4	N/A	N/A	0.5-.6 µm green	79 meters, 1.5 acres
5	N/A	N/A	0.6-.7 µm red	79 meters, 1.5 acres
6	N/A	N/A	0.7-0.8 µm IR	79 meters, 1.5 acres
7	N/A	N/A	0.8-1.1 µm IR	79 meters, 1.5 acres

Table 4: Landsat 4-7 Instruments and Bands

Band	TM Spectrum	TM Pixel Size	ETM+ Spectrum	ETM+ Pixel Size
1	0.45-0.52 µm blue	28.5 meters, 0.2 acres	0.45-0.52 µm blue	28.5 meters, 0.2 acres
2	0.52-0.6 µm green	28.5 meters, 0.2 acres	0.53-0.61 µm green	28.5 meters, 0.2 acres
3	0.63-0.69 µm red	28.5 meters, 0.2 acres	0.63-0.69 µm red	28.5 meters, 0.2 acres
4	0.76-0.9 µm NIR	28.5 meters, 0.2 acres	0.75-0.9 µm NIR	28.5 meters, 0.2 acres
5	1.55-1.75 µm SWIR	28.5 meters, 0.2 acres	1.55-1.75 µm SWIR	28.5 meters, 0.2 acres
6	10.4-12.5 µm TIR	120 meters, 3.6 acres	10.4-12.5 µm TIR	57 meters, 0.9 acres
7	2.08-2.35 µm SWIR	28.5 meters, 0.2 acres	2.1-2.35 µm SWIR	28.5 meters, 0.2 acres
8	N/A	N/A	0.52-0.9 µm panchromatic	14.25 meters, 0.05 acres

NB, IR = infrared; NIR = near infrared; SWIR = short wavelength infrared; TIR = thermal infrared (long wavelength); and µm = micron or micrometer.

Table 5: Landsat Scenes, Sensor and Date of Acquisition

Date	Sensor	Month of Acquisition
20_10_1984	TM5	October
21_11_1984	TM5	November
18_11_1986	TM5	November
30_11_1990	TM5	November
7_11-1999	TM5	November
09_11_2000	TMa5	November
27_10_2001	TM5	October
30_10_2002	TM%	October

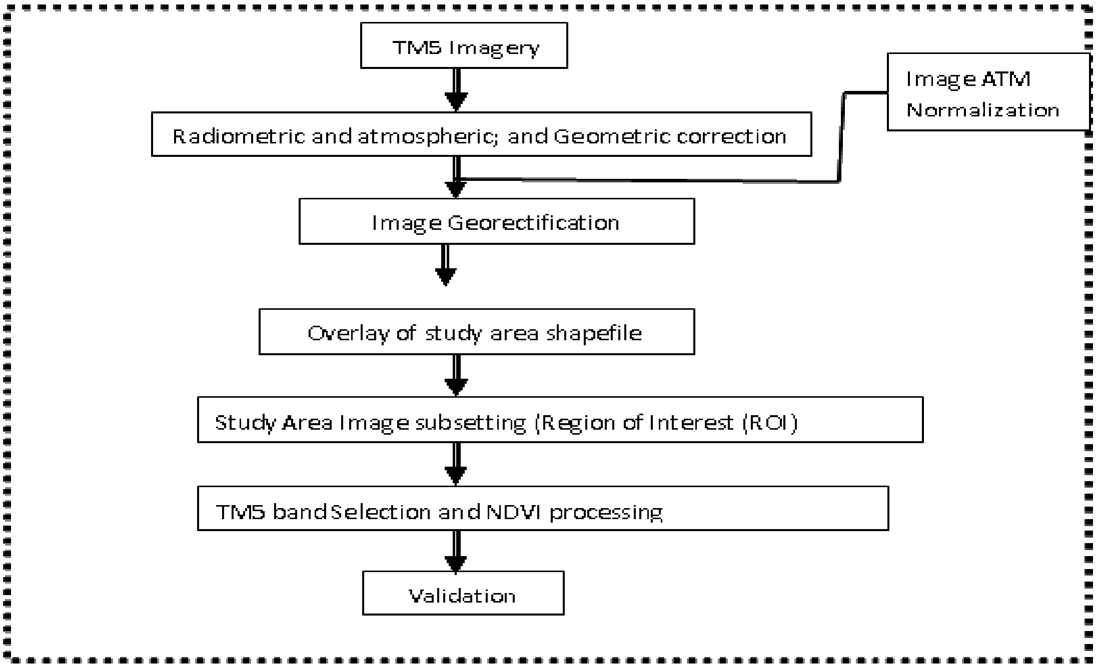

Figure 2: Steps for Image Processing

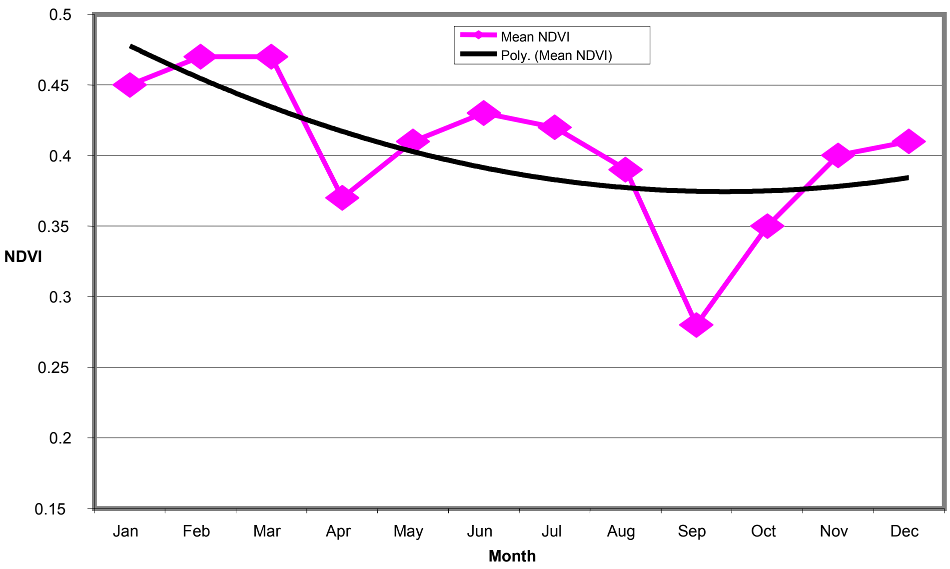

Figure 3: Mean Monthly NDVI for Africa (1982-2007)

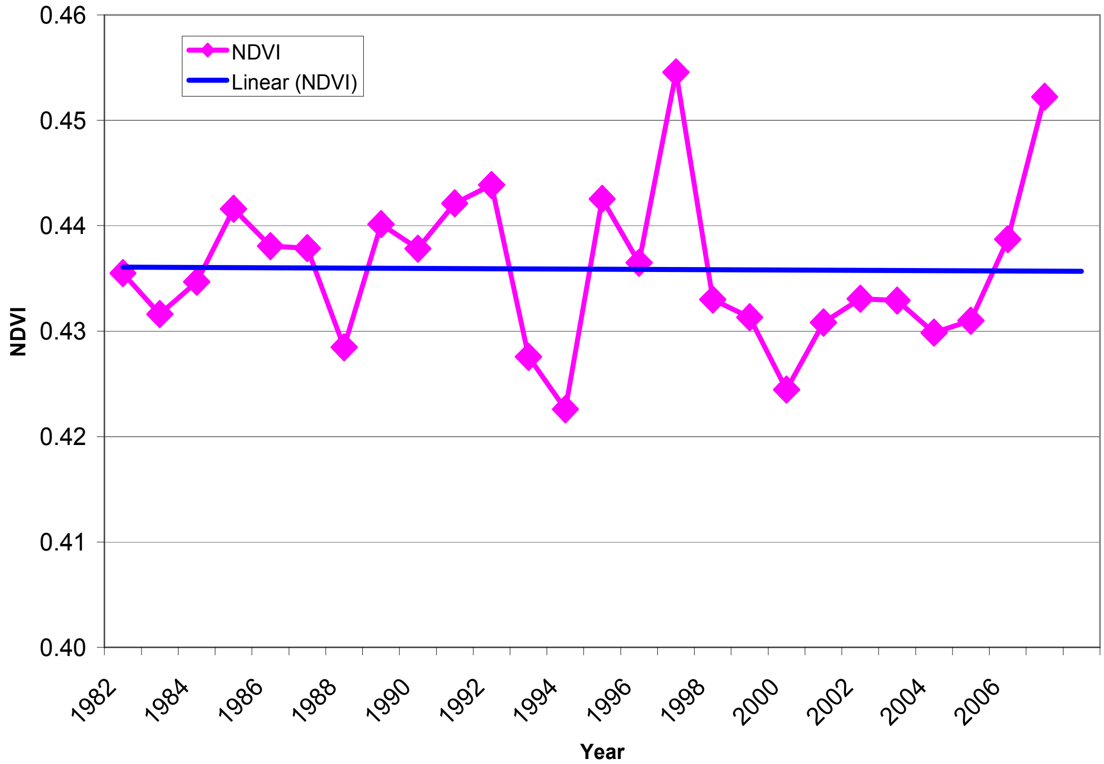

Figure 4: Mean Annual NDVI Trend for Africa between 1982 and 2007.

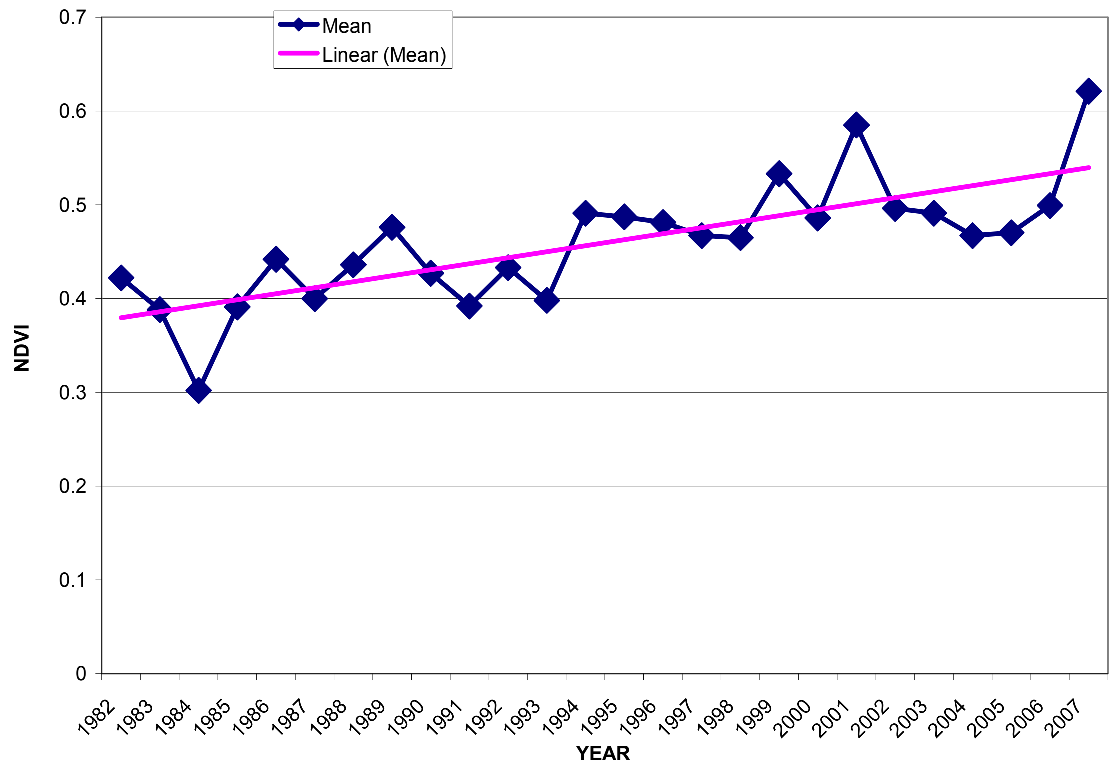

Figure 5: Mean Annual Mean NDVI for Sahel (1982-2007)

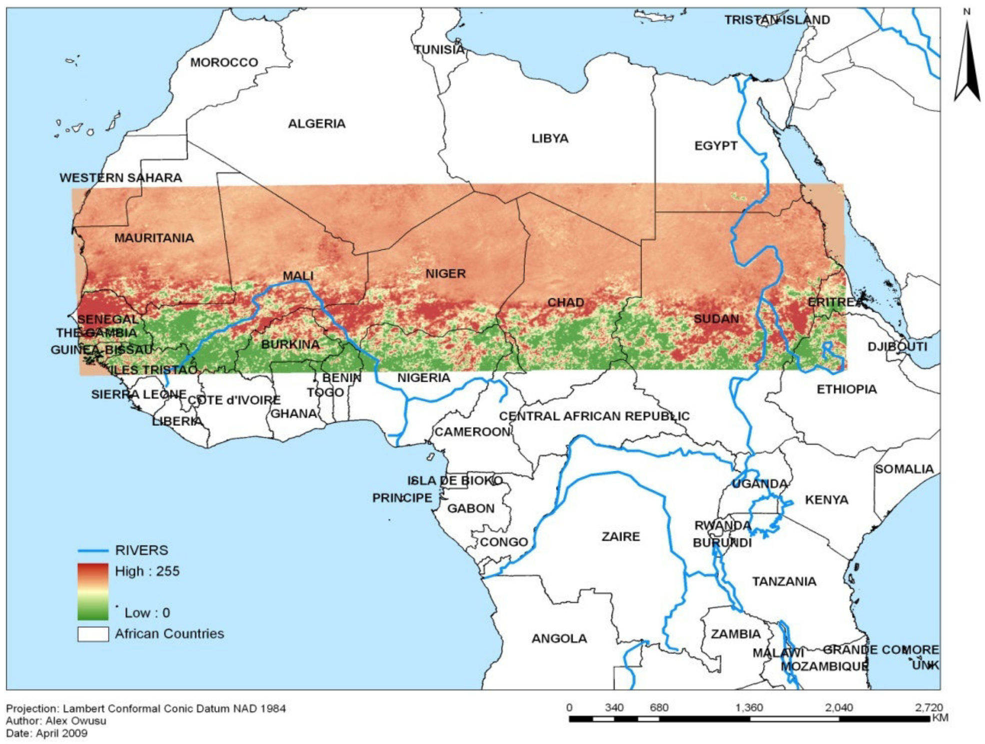

Figure 6: Mean Spatial Pattern of Land Degradation

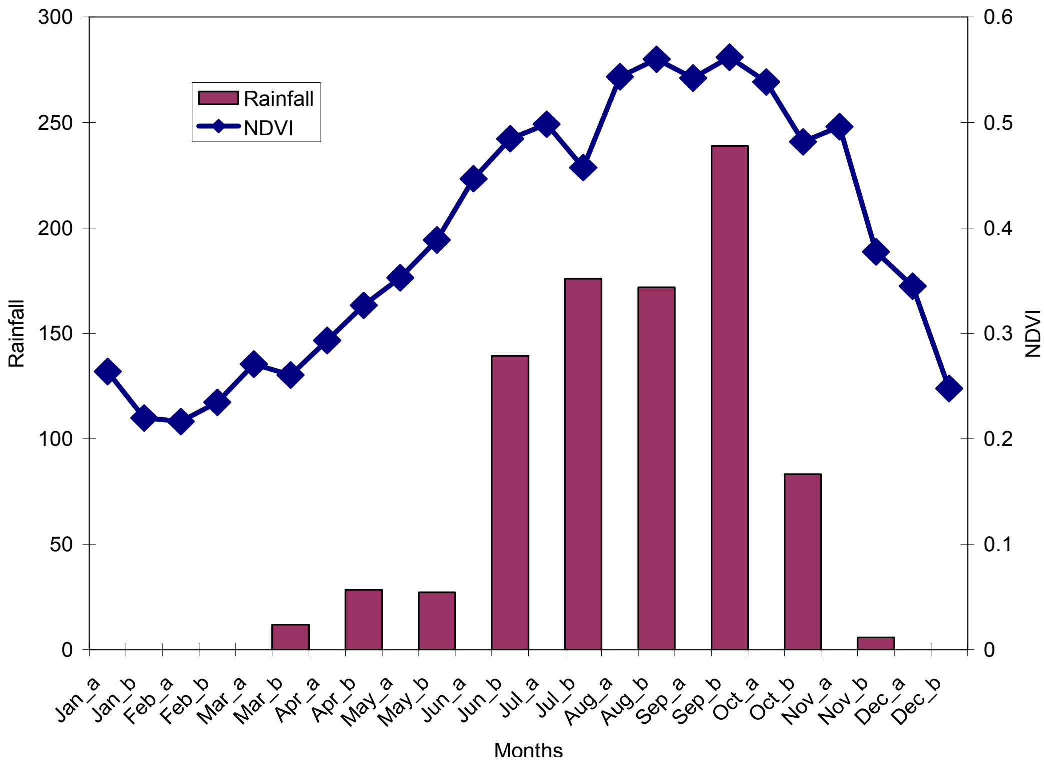

Figure 7: Normal Yearly NDVI Corresponding to Normal Rainfall of a Normal Year

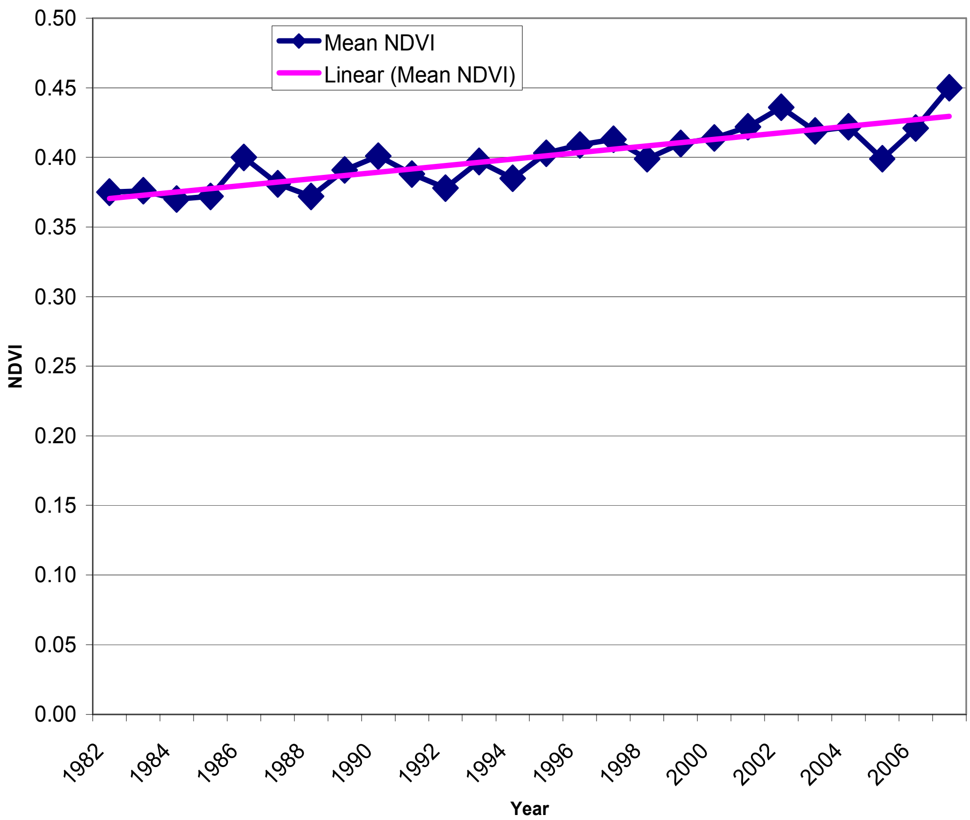

Figure 8: Mean NDVI for the UER 1982-2007

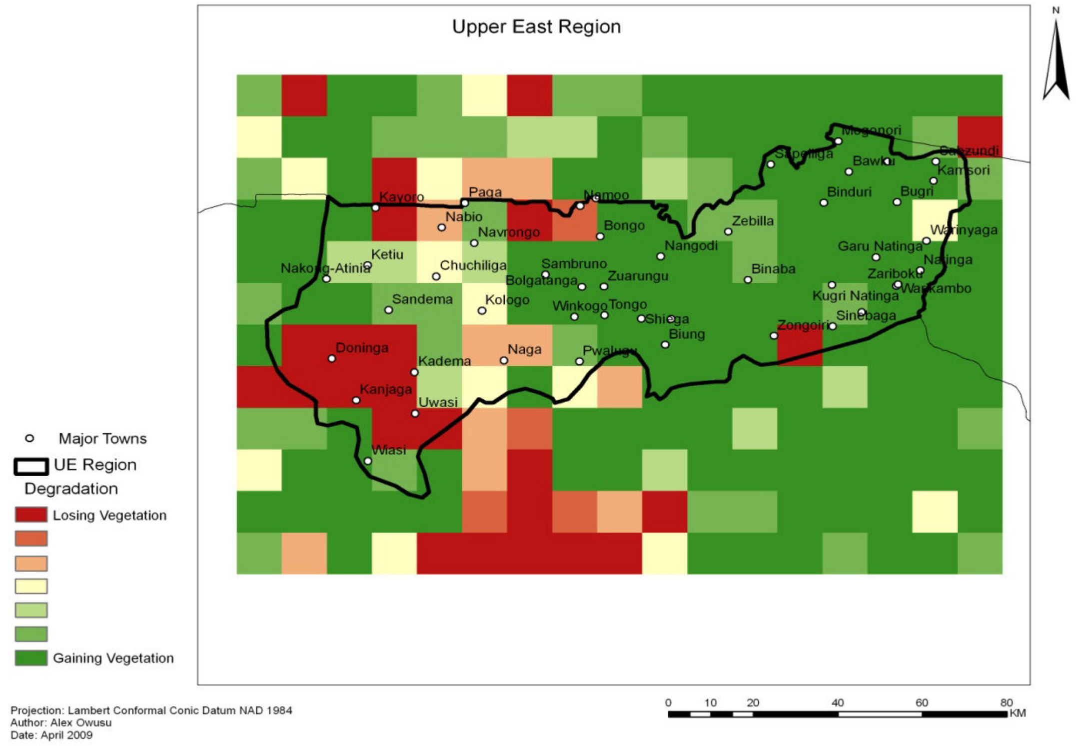

Figure 9: Mean Spatial Pattern of Land Cover Change

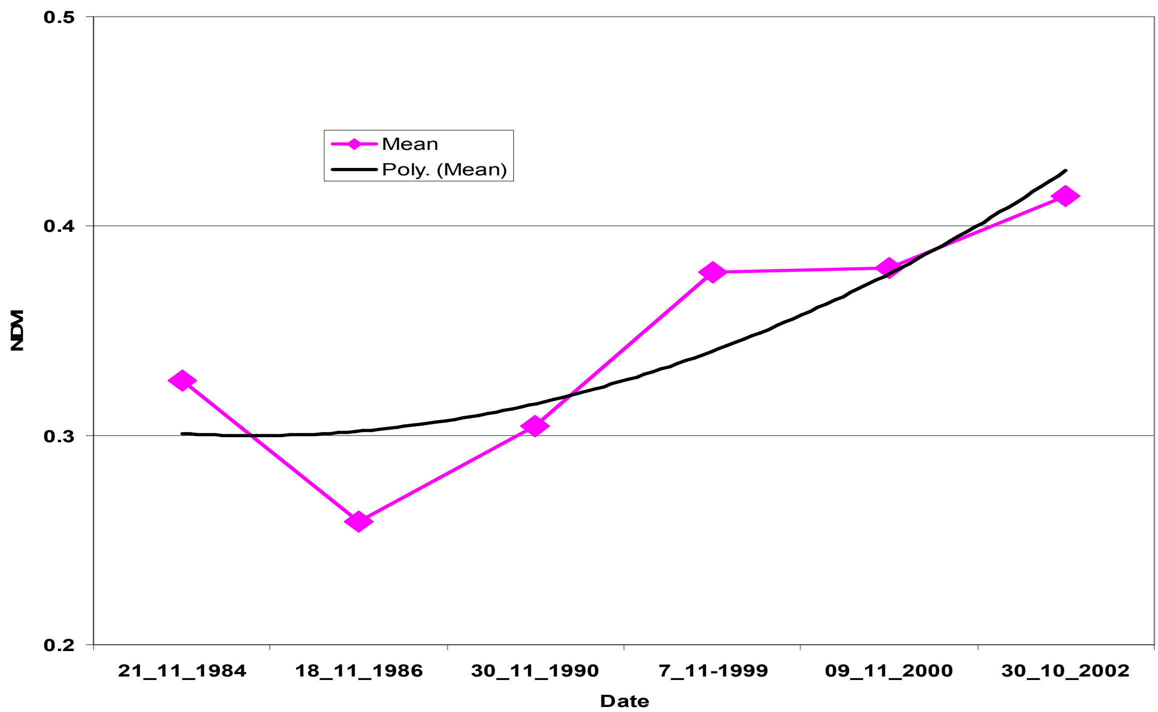

Figure 10: LTM5 Mean NDVI for October/November in the UER (1984-2002)

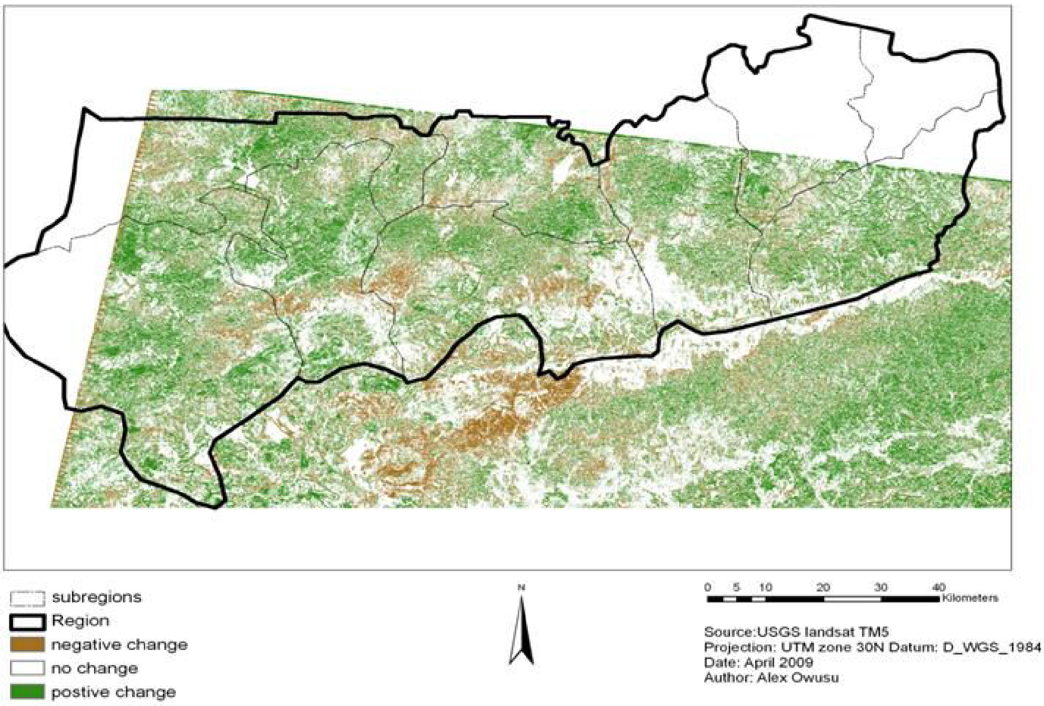

Figure 11: Spatial Degradation Detected from LTM5 NDVI